JOURNAL OF BACTERIOLOGY, Aug. 1995, p. 4748–4756
0021-9193/95/$04.00+0

Vol. 177, No. 16

Effects of Elemental Sulfur on the Metabolism of the Deep-Sea Hyperthermophilic Archaeon *Thermococcus* Strain ES-1: Characterization of a Sulfur-Regulated, Non-Heme Iron Alcohol Dehydrogenase

KESEN MA,[1,2] HOLGER LOESSNER,[1,2] JOHANN HEIDER,[1,2] MICHAEL K. JOHNSON,[2,3] AND MICHAEL W. W. ADAMS[1,2]*

Department of Biochemistry and Molecular Biology,[1] Center for Metalloenzyme Studies,[2] and Department of Chemistry,[3] University of Georgia, Athens, Georgia 30602

Received 6 February 1995/Accepted 6 June 1995

The strictly anaerobic archaeon *Thermococcus* strain ES-1 was recently isolated from near a deep-sea hydrothermal vent. It grows at temperatures up to 91°C by the fermentation of peptides and reduces elemental sulfur (S^0) to H_2S. It is shown here that the growth rates and cell yields of strain ES-1 are dependent upon the concentration of S^0 in the medium, and no growth was observed in the absence of S^0. The activities of various catabolic enzymes in cells grown under conditions of sufficient and limiting S^0 concentrations were investigated. These enzymes included alcohol dehydrogenase (ADH); formate benzyl viologen oxidoreductase; hydrogenase; glutamate dehydrogenase; alanine dehydrogenase; aldehyde ferredoxin (Fd) oxidoreductase; formaldehyde Fd oxidoreductase; and coenzyme A-dependent, Fd-linked oxidoreductases specific for pyruvate, indolepyruvate, 2-ketoglutarate, and 2-ketoisovalerate. Of these, changes were observed only with ADH, formate benzyl viologen oxidoreductase, and hydrogenase, the specific activities of which all dramatically increased in cells grown under S^0 limitation. This was accompanied by increased amounts of H_2 and alcohol (ethanol and butanol) from cultures grown with limiting S^0. Such cells were used to purify ADH to electrophoretic homogeneity. ADH is a homotetramer with a subunit M_r of 46,000 and contains 1 g-atom of Fe per subunit, which, as determined by electron paramagnetic resonance analyses, is present as a mixture of ferrous and ferric forms. No other metals or acid-labile sulfide was detected by colorimetric and elemental analyses. ADH utilized NADP(H) as a cofactor and preferentially catalyzed aldehyde reduction. It is proposed that, under S^0 limitation, ADH reduces to alcohols the aldehydes that are generated by fermentation, thereby serving to dispose of excess reductant.

Hyperthermophiles are a recently discovered group of microorganisms that have the remarkable property of growing at temperatures of 90°C and above (1, 2, 64, 65). They have been isolated from a variety of geothermally heated environments, and almost all are classified as *Archaea* (formerly *Archaeobacteria* [75]). The majority are strict anaerobes, and most are obligately dependent upon the reduction of elemental sulfur (S^0) to H_2S for optimal growth. Various organic compounds and molecular H_2 serve as electron donors for the apparent respiration of S^0. The mechanism of S^0 reduction in one autotrophic hyperthermophile, *Pyrodictium brockii*, an obligate S^0-reducing species which grows optimally at 105°C, has been investigated. This organism was shown to have a primitive membrane-bound electron transport chain for coupling H_2 oxidation and H_2S production (52), although the S^0-reducing entity was not purified.

On the other hand, some of the heterotrophic hyperthermophiles are able to grow well in the absence of S^0. These have fermentative-type metabolisms and produce H_2 during growth, although they also produce H_2S if S^0 is added to the growth medium. S^0 reduction was thought to be a mechanism of detoxifying inhibitory H_2 (23), but a more recent study showed that H_2S production plays a role in energy conservation by an as yet unknown mechanism (62). The best studied of the hyperthermophiles that are not obligately S^0 dependent is *Pyrococcus furiosus*, which grows optimally at 100°C (23). This organism contains two distinct S^0-reducing enzymes, both of which are cytoplasmic. These are an Ni-containing hydrogenase, now referred to as sulfhydrogenase (42), and a novel iron-sulfur flavoprotein termed sulfide dehydrogenase (39). The true substrates for S^0 reduction by these enzymes, as well as those in other hyperthermophilic species, are soluble polysulfides. These are generated from S^0, which is virtually insoluble in aqueous media, by its reaction with sulfide (13, 60, 61).

Little is known about the metabolic pathways that provide reductant for S^0 reduction by the heterotrophic hyperthermophiles, either in the S^0-dependent species or in those able to grow in its absence. In addition, the extent to which S^0 can influence or regulate the metabolism of these organisms remains an unanswered question. To address such issues, we have investigated the effect of S^0 on the growth and enzymatic activities of a novel deep-sea hyperthermophilic organism, isolate ES-1 (53). This organism was isolated from a polychaete worm (genus *Paralvinella*) whose only known habitat is the sulfide-rich walls of black smoker chimneys. Analysis of the 16S rRNA sequence of ES-1 has indicated that it is a member of the genus *Thermococcus* (7). This organism grows at temperatures up to 91°C and is an obligately anaerobic heterotroph that reduces S^0 and utilizes proteinaceous materials (peptone, yeast extract, and casein), but not carbohydrates, as

* Corresponding author. Mailing address: Department of Biochemistry, Life Sciences Bldg., University of Georgia, Athens, GA 30602. Phone: (706) 542-2060. Fax: (706) 542-0229. Electronic mail address: ADAMSM@BSCR.CC.UGA.EDU.

a carbon source (53). To date, there have been no reports concerning enzymes purified from ES-1.

We have previously characterized several enzymes involved in the primary metabolic pathways of two other heterotrophic hyperthermophiles, *Thermococcus litoralis* (T_{max}, 98°C [50]) and *P. furiosus* (1, 2). However, in contrast to these organisms, ES-1 does not utilize carbohydrates and, as we show herein, is obligately dependent upon S^0 reduction for growth. The initial objectives of this study were therefore (i) to examine ES-1 for the activities of a variety of enzymes previously detected in *P. furiosus* and *T. litoralis* that are postulated to be involved in peptide utilization and reductant generation and (ii) to determine if any of the activities were affected by S^0 limitation. Among the enzymes of interest were formaldehyde ferredoxin oxidoreductase (FOR) (48), aldehyde ferredoxin oxidoreductase (AOR) (47), hydrogenase (16), alcohol dehydrogenase (ADH) (41), glutamate dehydrogenase (GDH) (57), various dehydrogenases that use amino acids and formate as substrates, and several ferredoxin-linked oxidoreductases. The latter use the transaminated forms of amino acids as substrates and convert them to the acyl coenzyme A (acyl-CoA) thioester derivative. The substrates (and enzymes) are pyruvate (pyruvate oxidoreductase [POR]) (10), aryl pyruvates (indolepyruvate oxidoreductase [IOR]) (45), 2-ketoglutarate (2-ketoglutarate oxidoreductase [KGOR]) (2, 44), and branched-chain keto acids (2, 29).

On the basis of this study we have identified two novel enzymes in *Thermococcus* strain ES-1, a non-heme iron-containing ADH and a formate ferredoxin oxidoreductase (FMOR). Moreover, the activities of both of these enzymes, together with that of hydrogenase, were dramatically affected by the concentration of S^0 in the growth medium. Herein we describe the purification and characterization of ES-1 ADH, while the properties of FMOR will be described elsewhere (27). We also propose a pathway to explain the apparent regulation by S^0 of key enzymatic activities in this hyperthermophile.

MATERIALS AND METHODS

Growth of organism. *Thermococcus* strain ES-1 (hereafter referred to as ES-1) was obtained from John Baross of the University of Washington (53). It was routinely grown under Ar at 81°C as closed static cultures (50 ml) in serum-stoppered glass bottles (100 ml) by using a medium containing the following (per liter): NH_4Cl, 1.2 g; NaCl, 13.8 g; $MgSO_4$, 3.5 g; $MgCl_2$, 2.75 g; KCl, 0.325 g; $CaCl_2$, 0.75 g; KH_2PO_4, 0.5 g; NaBr, 0.05 g; H_3BO_4, 0.015 g; $SrCl_2$, 0.0075 g; sodium citrate, 0.005 g; KI, 0.05 g; tryptone, 5 g; yeast extract, 5 g; and resazurin, 0.5 mg. A mineral solution (10 ml/liter) (which contained [per liter] nitriloacetic acid, 1.0 g; $FeCl_3$, 1.1 g; $MnSO_4$, 0.5 g; $NiCl_2$, 0.2 g; $CoSO_4$, 0.1 g; $ZnSO_4$, 0.1 g; $CuSO_4$, 0.01 g; Na_2MoO_4, 0.01 g; and Na_2WO_4, 0.5 g,) was also added. The pH was adjusted to 6.5 prior to autoclaving. S^0 (sublimed sulfur powder; J. T. Baker, Phillipsburg, N.J.) was sterilized separately and was added to the hot sterile medium. It was routinely used at 15 g/liter for 50-ml cultures. Before inoculation, titanium chloride (0.5% [wt/vol] in 2 mM nitriloacetate, pH 5.0) was added (1.0 ml/liter of medium) to reduce resazurin. For large-scale cultures, two 20-liter cultures served as an inoculum for growth in a 600-liter fermentor wherein the culture was maintained at 81°C, bubbled with Ar (5 liters/min), and stirred (50 rpm). Cells were harvested with a Sharples centrifuge at 100 liters/h. They were immediately frozen in liquid N_2 and stored at −80°C. Cell growth was monitored by direct microscopic cell count and by the optical density at 600 nm (OD_{600}), after culture samples were first allowed to stand for 5 min so that unused S^0 would settle. An OD_{600} value of 1.0 corresponded to ca. 4 g (wet weight) per liter. To determine fermentation products, aliquots of the liquid or gas phase of 50-ml cultures were analyzed at the end of exponential growth for H_2 by gas chromatography (16) and for H_2S by methylene blue formation (18). The amounts of various organic compounds were determined with a Varian 3300 gas chromatograph fitted with a flame ionization detector and a fused silica Nukol column (0.53 mm by 15 m; Supelco, Bellefonte, Pa.). The column, injector, and detector temperatures were 120, 220, and 220°C, respectively.

Enzyme assays. Frozen cells of ES-1 were thawed anaerobically in approximately 3 volumes of 50 mM Tris-HCl buffer, pH 7.8, containing lysozyme (1 mg/ml), DNase (10 μg/ml), 2 mM sodium dithionite, and 2 mM dithiothreitol and were incubated at 37°C for 4 h with constant stirring. Cell lysis by this procedure was confirmed by microscopic examination. A cell extract was obtained by centrifugation at 50,000 × *g* for 80 min at 4°C, and this was used directly for determining enzymatic activities. All assays were carried out under anaerobic conditions at 80°C. The activities of POR, IOR, KGOR, and 2-ketoisovalerate oxidoreductase (VOR) were determined by measuring the substrate-dependent reduction of methyl viologen in the presence of CoA with pyruvate, indolepyruvate, 2-ketoglutarate, or 2-ketoisovalerate as the substrate (final concentration, 5 mM), respectively (11, 45). AOR, FOR, and FMOR activities were measured by the CoA-independent reduction of benzyl viologen. Crotonaldehyde (47) and formaldehyde (48) were used as substrates for AOR and FOR, respectively. For FMOR, the assay was the same as for AOR except that formate (1 mM) was used as the substrate. Hydrogenase activity was measured both by the H_2-dependent reduction of methyl viologen and by H_2 evolution from reduced methyl viologen (16). The activities of GDH and ADH were measured by the glutamate-dependent reduction and the ethanol-dependent reduction of NADP, respectively, as previously described (41). The substrate specificity and kinetic parameters of purified ADH were determined by the same assay procedure except that the substrates and electron carriers were varied as described in Results. Acetyl coenzyme A (acetyl-CoA) reductase activity of ADH was measured as described previously (33) except that the assay temperature was 80°C. The activities of formate dehydrogenase, alanine dehydrogenase (AlaDH), leucine dehydrogenase (LeuDH), valine dehydrogenase (ValDH), and phenylalanine dehydrogenase (PheDH) were measured by the NADP-dependent assay for GDH (41) except that the corresponding amino acid (final concentration, 5 mM) or formate (10 mM) replaced glutamate. For all of the enzymes listed above, 1 U of activity represents 1 μmol of substrate oxidized per min. The exception is hydrogenase, for which 1 U equals 1 μmol of H_2 produced per min in the evolution assay and 1 μmol of H_2 oxidized per min in the uptake assay. The pH dependence of ADH activity was measured by using 100 mM EPPS [*N*-(2-hydroxyethyl)piperazine-*N*′-3-propanesulfonic acid; pH 7.2 to 8.8], 50 mM glycine–NaOH (pH 9.5), and 50 mM CAPS [3-(cyclohexylamino)-1-propanesulfonic acid; pH 10.5 to 11.1]. All pH values were measured at 23°C. The effect of temperature on ADH activity was measured by using 100 mM EPPS (pH 8.8).

Enzyme purification. ADH was routinely purified from 500 g (wet weight) of ES-1 cells under anaerobic conditions (16) at 23°C. A cell extract (1.2 liters) was prepared as described above and was loaded onto a column (8 by 21 cm) of DEAE-Sepharose Fast Flow (Pharmacia LKB, Piscataway, N.J.) equilibrated with buffer A (50 mM Tris-HCl [pH 7.8] containing 10% [vol/vol] glycerol, 2 mM dithiothreitol, and 2 mM sodium dithionite). The column was eluted with a 6.8-liter linear 0 to 0.8 M KCl gradient in buffer A. The flow rate was 8.5 ml/min, and 100-ml fractions were collected. ADH activity started to elute from the column as 0.3 M KCl was applied. Fractions containing ADH activity above 5.0 U/mg were combined (600 ml) and loaded onto a column (5 by 12 cm) of hydroxyapatite (Bio-Rad) equilibrated with buffer A lacking sodium dithionite (buffer B). The flow rate was 3 ml/min, and 100-ml fractions were collected. The column was eluted with a 1.8-liter linear 0 to 0.25 M potassium phosphate gradient in buffer A. The ADH activity started to elute as 0.08 M potassium phosphate was applied to the column. Fractions containing ADH activity above 20 U/mg were combined (700 ml), concentrated by ultrafiltration with Amicon type PM-30 membrane, and then washed with 10 volumes of buffer B. The concentrated fraction (27 ml) was applied to a column of Superdex 200 (6 by 60 cm; Pharmacia LKB) equilibrated with buffer B containing 50 mM KCl. The flow rate was 3 ml/min, and 30-ml fractions were collected. Those fractions containing pure ADH as judged by electrophoretic analysis (see below) were combined (90 ml), concentrated by ultrafiltration to 15 ml, and stored as pellets in liquid N_2.

Other methods. The molecular weight of ADH was estimated by gel filtration on a column of Superdex 200 (1.6 by 60 cm; Pharmacia LKB) with ferritin (molecular weight, 450,000), catalase (240,000), lactate dehydrogenase (140,000), yeast alcohol dehydrogenase (150,000), bovine serum albumin (67,000), and egg albumin (45,000) as the standard proteins. Sodium dodecyl sulfate (SDS)-polyacrylamide gel electrophoresis was performed on 12.5% polyacrylamide gels by the method of Laemmli (34). SDS molecular weight markers were purchased from Sigma Chemical Co. (St. Louis, Mo.). Protein concentrations were routinely estimated by the method of Bradford (15) with bovine serum albumin as the standard. The protein content of samples of pure ADH was also determined by the quantitative recovery of amino acids from compositional analyses (see below). Amounts of protein (determined by the sum of amino acids) in all samples were 84% ± 2% of those measured by the colorimetric protein assay (from three separate determinations). All analytical values for the pure protein that were based on the Bradford method have therefore been corrected by a factor of 0.84. A complete metal analysis (40 elements, including zinc and iron) was performed by plasma emission spectroscopy using a Jarrel Ash Plasma Comp 750 instrument at the Center for Complex Carbohydrate Research, University of Georgia. The iron and acid-labile sulfide contents of pure ADH were measured by using *o*-phenanthroline (38) and by methylene blue formation (18). The N-terminal sequence was determined with an Applied BioSystems model 477 sequencer (20). Amino acid analyses were performed with an Applied BioSystems model 4240A analyzer after hydrolysis of the protein under Ar at 165°C for 1 h in the presence of a solution containing 6 M HCl, 1% (wt/vol) phenol, and 8% (wt/vol) thioglycolic acid. The serine and threonine levels were corrected for destruction. Apoprotein was prepared and reduced with dithiothreitol under anaerobic conditions by previously described methods (4). The cysteine content of the reduced apoprotein was estimated from the apoprotein's reaction with

TABLE 1. Metabolic products of ES-1 grown with high and low S^0 concentrations[a]

S^0 concn (g/liter)	Final cell density (OD_{600})[b]	Concn of organic product (μM)[c]					H_2 concn (nmol/ml)[c,d]	H_2S concn (μM)[c]
		Acetate	Isovalerate	Isobutyrate/propionate[e]	Butyrate	Ethanol/butanol[e]		
1.0	0.29	644 ± 20	141 ± 7	52 ± 4	3.0 ± 1.0	49.4 ± 15.0	166 ± 16	4,340 ± 180
15.0	0.44	1,420 ± 40	411 ± 15	54 ± 4	8.0 ± 2.0	13.0 ± 5.0	8 ± 2	13,700 ± 300

[a] At the end of exponential growth, aliquots were removed from the media and organic products and H_2S were measured. The gas phase was also sampled to determine the H_2 concentration. All analytical results represent the average values from three separate determinations.
[b] OD_{600}, optical density at 600 nm.
[c] Data are averages ± standard deviations.
[d] H_2 concentration is expressed as nanomoles of H_2 in the gas phase per milliliter of culture medium.
[e] The organic products ethanol and butanol and the organic products isobutyrate and propionate could not be distinguished under the experimental conditions.

5,5′-dithiobis-(2-nitrobenzoic acid) (56). The tryptophan content was determined by the method of Edelhoch (22). The melting temperature of pure ADH was measured with a differential scanning calorimeter (Hart Scientific, Pleasant Grove, Utah). Protein concentrations were 2.3 and 4.2 mg/ml in 20 mM glycylglycine (pH 8.25) containing 2 mM dithiothreitol, and the scan rate was 60°C/h. Electron paramagnetic resonance (EPR) spectra were recorded on an IBM-Bruker ER 300D spectrometer interfaced to an ESP 3220 Data System and equipped with an Oxford Instruments ITC-4 flow cryostat.

RESULTS

Effect of S^0 on cell growth and metabolism. ES-1 grew well in a medium containing S^0 (15 g/liter) as a terminal electron acceptor with proteinaceous material (yeast extract and tryptone) as the sole C source, as previously reported (53). Cell doubling times in 50-ml static cultures were approximately 2 h, and densities approached 5×10^8 cells per ml. No growth was observed when the yeast extract and tryptone were replaced by maltose or starch (0.5% [wt/vol]), consistent with the earlier conclusion that ES-1 is obligately proteolytic (53). However, in contrast to the previous study (53), in our experiments little if any growth of ES-1 was observed if S^0 was omitted from the medium, even when the gas phase was sparged with Ar to prevent accumulation of H_2, a potential growth inhibitor. The small amount of growth that was observed was due to the transfer of some S^0 with the inoculum, as upon a second transfer into S^0-free media, no cell growth was detected (in contrast to the case with the S^0-containing control) as monitored by optical density and cell counting. In small-scale cultures, optimal growth required S^0 at a concentration of approximately 5 g/liter (data not shown). When the concentration was reduced to 1.0 g/liter, both the growth rate and the final cell density decreased by approximately 40%. Moreover, a similar dependence upon S^0 was seen when ES-1 was grown in a fermentor. For example, cell yields (wet weight) from 600-liter cultures with media containing 1.0, 0.04, and 0.01 g of S^0 per liter were approximately 1.9, 0.8, and 0.4 kg, respectively. Note that much lower S^0 concentrations were required to limit growth under these conditions, presumably because the large-scale cultures were both stirred and continually flushed with Ar, in contrast to the small-scale static cultures. No attempt was made to quantitatively correlate cell yield with the amount of S^0 utilized (either in the fermentor or in static cultures) because of the inherent difficulties in accurately measuring unreacted S^0, polysulfide, and sulfide (as HS^-, H_2S, insoluble metal sulfides, etc.) in the complex and highly reducing growth medium.

To investigate the metabolic effects of limiting the S^0 concentration during growth of ES-1, 50-ml static cultures were grown by using media containing either 15 or 1.0 g of S^0 per ml, and the fermentation products were analyzed at the end of the exponential growth phase. As shown in Table 1, the predominant metabolic products under high-S^0 conditions were acetate and isovalerate, together with large amounts of sulfide (approaching 14 mM). Small amounts of alcohol (ethanol plus butanol) were also produced, but the alcohol-to-acetate ratio was only about 0.01. When the S^0 concentration was lowered (to 1 g/liter), the amount of acetate produced decreased to less than half of that produced under high-S^0 conditions while the acetate/ethanol (plus butanol) ratio increased almost 10-fold. Similarly, the shift from a high to a low S^0 concentration dramatically increased the amount of H_2 produced, such that the H_2-to-H_2S ratio increased approximately 65-fold (Table 1). S^0 limitation therefore appeared to cause a shift in fermentation products, with an increase in H_2 and alcohol production and a decrease in the amounts of acids and H_2S produced.

Since a change in the pattern of metabolic products implied some form of regulation, the activities of some key oxidoreductase-type enzymes involved in amino acid degradation and fermentative-type processes were examined in cell extracts of ES-1. In this case cells were grown in a 600-liter fermentor under high (1.5 g/liter)- and low (0.04 g/liter)-S^0 regimens. As shown in Table 2, extracts contained high activities of GDH, of the two aldehyde-oxidizing enzymes AOR and FOR, and of four enzymes that oxidize the transaminated forms of amino acids to the CoASH derivative, IOR, KGOR, VOR, and POR. However, while there were some variations, none of these enzymes showed dramatic changes in specific activity in response to the change in S^0 concentration. Extracts of ES-1 cells also contained measurable AlaDH activity (Table 2), although the activities of ValDH, LeuDH, and PheDH were barely

TABLE 2. Effect of S^0 concentration on the activities of oxidoreductase-type enzymes in ES-1[a]

Enzyme (assay)[b]	Sp act (U/mg)[c]		Ratio[d]
	High S^0	Low S^0	
ADH	0.024 ± 0.008	0.44 ± 0.21	18
FMOR	0.14 ± 0.02	4.64 ± 0.84	33
H2ase (evolution)	<0.1	1.33 ± 0.52	>133
H2ase (oxidation)	0.28 ± 0.02	6.2 ± 0.46	22
GDH	3.58 ± 0.54	6.95 ± 0.18	1.9
AlaDH	0.093 ± 0.010	0.131 ± 0.021	1.4
AOR	4.46 ± 0.21	2.58 ± 0.05	0.6
FOR	2.56 ± 0.64	4.35 ± 1.54	1.7
POR	5.65 ± 0.66	8.70 ± 0.42	1.5
IOR	2.54 ± 0.11	1.32 ± 0.20	0.5
KGOR	2.16 ± 0.13	1.31 ± 0.21	0.6
VOR	3.88 ± 0.24	2.54 ± 0.36	0.7

[a] All activities were measured at 80°C as described in Materials and Methods, and data represent the average values from three separate determinations.
[b] Hydrogenase (H2ase) activity was measured by both H_2 evolution and H_2 oxidation assays.
[c] Data are averages ± standard deviations. High and low S^0 correspond to S^0 concentrations of 1.5 and 0.4 g/liter, respectively.
[d] Ratio of activities in low-S^0 cells to those in high-S^0 cells.

TABLE 3. Purification of ADH of ES-1

Step	Amt of protein (mg)	Activity (U)	Sp act (U/mg)	Yield (%)	Purification (fold)
Cell extract	3,120	21,500	6.7	100	1
DEAE FF[a]	1,200	14,280	11.9	66	1.8
Hydroxyapatite	424	16,400	38.8	77	5.8
Superdex 200	180	9,580	53.2	45	7.9

[a] FF, Fast Flow.

detectable (<0.01 U/mg). Again, there was no major effect on the activities of these enzymes when the S^0 concentration was decreased. We were unable to detect any formate dehydrogenase activity [using NAD(P) as the electron acceptor] in cell extracts, but an enzyme that catalyzed the formate-dependent reduction of benzyl viologen, indicative of FMOR, was present (Table 2). Moreover, the activities of FMOR, ADH, and hydrogenase increased 20-fold or more upon reduction of the S^0 concentration (Table 2). In fact, the activities of all three enzymes were difficult to detect in extracts of cells grown in the presence of a high S^0 concentration. Remarkably, the activities of ADH and FMOR (and to a lesser extent, hydrogenase), increased even further when the S^0 concentration was reduced in the fermentor from 0.04 to 0.01 g/liter. Typical values (in units per milligram) for ADH, FMOR, and hydrogenase were 5.0 (from 0.44), 105 (from 4.6), and 3.8 (from 1.3), respectively. On the other hand, the activities of the other enzymes listed in Table 2 were not significantly affected (data not shown). Thus, we conclude that the increase in H_2 and alcohol production under limiting S^0 concentrations is in some way related to the increased activities of these three enzymes. In the following paragraphs, we describe the purification and characterization of one of these, ADH, from cells grown in the presence of a low (0.01 g/liter) S^0 concentration.

Purification and physical properties of ADH. More than 90% of the ADH activity was found to be in the supernatant after centrifugation of the cell extract of ES-1, indicating that the enzyme is a cytoplasmic protein. The results of a typical purification are shown in Table 3. ADH was purified about eightfold with a yield of activity of 45%, indicating that it is a major cytoplasmic protein when cells are grown under S^0 limitation. The purified enzyme gave a single protein band after SDS-gel electrophoresis (Fig. 1), and this band corresponded to an M_r of 46,000. The apparent M_r of the native enzyme was 200,000 ± 20,000 as determined by gel filtration (data not shown). These results suggest that the enzyme has a homotetrameric structure. Amino-terminal sequence analysis of a solution of ADH gave rise to a single sequence (Fig. 2), consistent with the presence of a single type of subunit. A comparison of the N-terminal amino acid sequence of the ES-1 enzyme with those of the ADHs from methanogenic, aerobic, and hyperthermophilic archaea, from thermophilic and mesophilic bacteria, and from eucaryotes shows that it has significant sequence homology only to the enzyme from the hyperthermophile *T. litoralis* (41). However, the amino acid compositions of the two hyperthermophilic ADHs are quite distinct (Table 4). In particular, the ES-1 enzyme contained eight histidinyl residues and one methionyl residue compared with values of one and six, respectively, for the *T. litoralis* enzyme. ES-1 ADH was quite thermostable. The times required for a 50% loss in catalytic activity with the enzyme at a concentration of 11 mg/ml (in 50 mM EPPS [pH 8.0]) were about 35 h at 85°C and 4 h at 95°C. The ES-1 enzyme (2.3 mg/ml in 20 mM glycylglycine [pH 8.25]) gave a reasonably

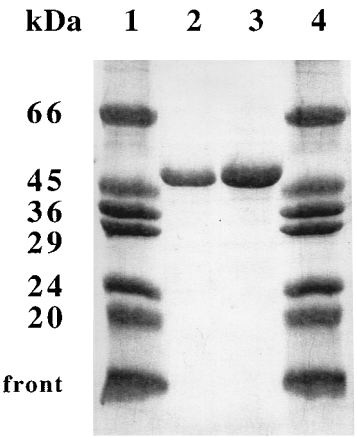

FIG. 1. SDS–12.5% (wt/vol) acrylamide electrophoresis gel of ADH purified from ES-1. Lanes 1 and 4, molecular mass markers; lanes 2 and 3, 2 and 4 μg of ADH, respectively.

symmetrical peak of thermal denaturation when analyzed by differential scanning calorimetry (data not shown) with a corresponding melting temperature of 105°C.

Pure ADH contained 0.95 ± 0.20 g-atom of Fe per subunit as measured by the colorimetric assay for iron. Analysis of the enzyme by plasma emission spectroscopy showed that no other metals were present in significant amounts (>0.1 g-atom per subunit), although the iron content was somewhat lower (0.65 ± 0.1 atom of Fe per subunit) when determined by this method. No acid-labile sulfide was detected in ADH. Solutions of pure ADH (purified anaerobically in the presence of dithiothreitol but not sodium dithionite) at high protein concentrations (~15 mg/ml) were slightly yellowish, and several distinct peaks were evident in the visible absorption spectrum (data not shown). This situation was unchanged after the sample was shaken in air and left exposed to air for 30 min. However, addition of sodium dithionite caused an approximately 50% decrease in absorption throughout the visible region (A_{600} per subunit of 0.31 $mM^{-1} \cdot cm^{-1}$). The pure enzyme and the dithionite-reduced form exhibited the same specific activity when assayed under standard conditions.

Analysis of ES-1 ADH by EPR spectroscopy indicated that the changes in visible absorption upon oxidation-reduction probably arose from a redox change at the iron site. That is, the enzyme as purified under anaerobic conditions but in the absence of sodium dithionite gave rise to an EPR resonance near g = 4.3, which is characteristic of high-spin ferric iron (Fig. 3A). Attempts to further oxidize the iron site by treating the

ES:	**M**	**L**	**W**	**E**	**S**	**Q**	**I**	**P**	**I**	**N**	**Q**	I	**F**	E	**L**	X	X	A	**T**	**I**	**D**
Tl:	**M**	**L**	**W**	**E**	**S**	G	L	**P**	**I**	**N**	**Q**	V	**F**	X	**L**	X	X	K	**T**	**I**	**D**
Zm:	A	S	S	T	F	Y	**I**	**P**	F	V	N	E	M	G	E	G	S	L	E	K	A
Dg:	-Q	V	Y	G	F	**F**	**I**	**P**	S	V	T	L	I	G	I	G	A	S	K	E	I
Tb:	**M**	K	G	F	A	M	L	S	**I**	G	K	V	G	W	I	E	K	E	K	P	A
Sc:	S	I	P	**E**	T	**Q**	K	G	V	I	F	Y	E	S	H	G	K	L	E	Y	K
Dm:	S	F	T	L	T	N	K	N	V	I	F	V	A	G	**L**	G	G	I	G	L	**D**
Ss:	**M**	R	A	V	R	L	V	E	**I**	G	K	P	L	S	**L**	Q	E	I	G	V	P
Ml:	**M**	E	T	K	V	G	Y	F	A	S	L	E	Q	Y	K	X	R	D	A	L	E

FIG. 2. Amino-terminal amino acid sequences of ADHs from various sources. The abbreviations used and the references are as follows: ES, ES-1 (this work); Tl, *T. litoralis* (41); Sc, *Saccharomyces cerevisiae* (9); Dm, *Drosophila melanogaster* (71); Tb, *Thermoanaerobium brockii* (51); Zm, *Z. mobilis* (adh2 [49]); Ss, *S. solfataricus* (3); Dg, *Desulfovibrio gigas* (30); Ml, *Methanogenium liminatans* (12); and X, unidentified residue. The 4 N-terminal residues of the Dg protein (A V R E −) are not shown. Residues identical to those in the ES-1 protein are in bold.

TABLE 4. Amino acid composition of ADHs from ES-1 and *T. litoralis*

Amino acid(s)	No. of residues in ADH from:	
	ES-1[a]	*T. litoralis*[b]
Asn + Asp	29	28
Gln + Glu	59	57
Ser	13	13
Gly	46	53
Arg	14	9
Thr	20	19
Ala	43	61
Pro	16	30
Tyr	5	17
Val	34	36
Met	1	6
Trp	8	11
Cys	2	3
Ile	14	39
Leu	58	52
Phe	17	4
Lys	39	15
His	8	1

[a] Calculated M_r of ADH, 46,193.
[b] Data taken from reference 41. Calculated M_r of ADH, 47,751.

enzyme (14 mg/ml in 50 mM Tris-HCl [pH 8.0]) at either 25 or 80°C (for up to 5 min) with air, potassium ferricyanide (5 mM), H_2O_2 (5% [vol/vol]), NADP (2 mM), or acetaldehyde (5 mM) were unsuccessful as monitored by EPR spectroscopy, i.e., no change in the EPR absorption was observed. However, the addition of the high-potential dye 2,6-dichlorophenol indophenol ($E_0' = +260$ mV) increased the intensity of the g = 4.3 signal, while the addition of sodium dithionite decreased its intensity (Fig. 3A). It therefore appeared that the iron in the pure enzyme was a mixture of ferric and ferrous forms. The presence of ferrous iron was confirmed by treatment of the pure enzyme with NO, which led to new EPR resonances at low magnetic field (Fig. 3B). These were in addition to an intense signal centered near g = 1.95 (data not shown), which arises from the NO radical (the same EPR absorption was seen in the absence of enzyme). The new resonances could be resolved into two distinct species with resonances at g = 4.28 and 9.46 and at g = 3.99, according to their temperature (Fig. 3C) and microwave power dependence (data not shown). The g = 3.99 resonance is characteristic of species with an $S = 3/2$ ground state and can be reasonably assigned to a ferrous NO complex (76), while the additional resonances (g = 4.28 and 9.46) were assumed to arise from the unreacted ferric site ($S = 5/2$). The latter assignment was confirmed by the addition of NO to the dithionite-reduced enzyme. As shown in Fig. 3A, the g = 3.99 signal from the ferrous NO complex then predominated, and the low-intensity resonance at g = ~4.3 was similar to that observed from the dithionite-reduced enzyme. This resonance presumably arises either from adventitiously bound ferric iron or from an inactive form of the active center. Quantitation of these different forms of mononuclear iron sites was not attempted. Nevertheless, we can conclude that the enzyme as prepared contains an iron site that is composed of approximately equal amounts of ferric and ferrous forms, together with a much smaller amount of "junk" iron. Both the ferrous form and the ferric form (after reduction by sodium dithionite) react with NO, but the ferrous form is resistant to oxidation by substrates, peroxide, ferricyanide, and O_2.

Catalytic properties of ADH. The enzyme catalyzed the oxidation of a range of aliphatic (C_2 to C_8) and aromatic primary alcohols at 80°C with NADP as the electron acceptor, but it did not oxidize methanol and showed little if any activity with polyols or hydroxycarboxylic acids (Table 5). NAD also functioned as an electron acceptor for ethanol oxidation, but the enzyme had an extremely low affinity for this cofactor (apparent K_m of ≥10 mM) compared with NADP (apparent K_m of 14 μM) (see Table 6). For ethanol oxidation at 80°C, the optimal pH was 8.8 to 10.4 with approximately 50% of the maximal activity at pH 8.3 and at pH 11.1. At pH 8.8, the activity increased with increasing temperature from 30°C (3 U/mg) to 95°C (102 U/mg) with an optimum above 95°C. The corresponding Arrhenius plot showed no obvious transition point over this temperature range. ADH also catalyzed the reduction of acetaldehyde and phenylacetaldehyde with NADPH as the electron donor. The enzyme had no detectable activity as an acetyl-CoA reductase, as was found with the ADH from *Escherichia coli* (19, 33). As shown in Table 6, although the maximal specific activities for aldehyde reduction and alcohol oxidation were comparable, the enzyme was much more efficient in catalyzing aldehyde reduction. That is, the apparent K_m values were less than 250 μM for both the aldehyde substrate and the cofactor (NADPH), compared with values of ≥8 mM for the alcohols examined. Clearly, the physiological role of ADH is more likely to be aldehyde reduction than alcohol oxidation, and NADP(H) rather than NAD(H) is the preferred cofactor. Additional analyses using ethanol (10 to 60 mM) and NADP (0.05 to 0.3 mM), in which the concentration of one substrate was varied (over the indicated range) and the concentration of the other was constant, gave rise to parallel Lineweaver-Burk plots (data not shown), indicating a ping-pong type of catalytic mechanism for alcohol oxidation. The addition of NaCl (0.3 mM), KCl (0.3 mM), or potassium phosphate (0.2 mM) to the assay medium stimulated the ethanol oxidation activity of ADH activity by about 20%, while the addition of $FeSO_4$ (0.2 mM), $(NH_4)_2SO_4$ (0.15 mM), cyanide (10 mM), azide (10 mM), CO (1 atm [101.29 kPa]), or EDTA (5 mM) had no significant effect and $ZnSO_4$ (0.5 mM) caused a decrease in activity of about 30%. After a solution of the enzyme was gently bubbled with NO for 3 min at 25°C, no ethanol oxidation activity could be detected under standard assay conditions at 80°C.

DISCUSSION

When grown under S^0-limiting conditions, the hyperthermophilic archaeon *Thermococcus* strain ES-1 contains very high concentrations of a cytoplasmic ADH. Its molecular and catalytic properties differ from those of the zinc-containing ADHs purified from other archaea, such as methanogens (12, 74) and the aerobe *Sulfolobus solfataricus* (55), but it is similar in molecular size, cofactor specificity, substrate specificity, and amino-terminal sequence to ADH from the hyperthermophilic archaeon *T. litoralis* (41). Although the *T. litoralis* enzyme was reported not to contain significant amounts of any metal (41), more recent studies have shown that a more rapid and smaller-scale purification procedure for *T. litoralis* ADH yields an enzyme with an iron content of 0.1 to 0.5 g-atom per subunit with corresponding increases in specific activity (40). This suggests that *T. litoralis* ADH is also an iron-containing enzyme but that it loses iron during purification. A diverse multitude of microbial NAD(P)-dependent ADHs are known to exist (recently reviewed in reference 54), but only a limited number fall into the so-called group III family, the members of which are characterized by their primary structure and subunit size and by a requirement for a divalent metal ion for activity (21, 24, 26, 30, 33, 73). Of these, only the enzymes from *Zymomonas*

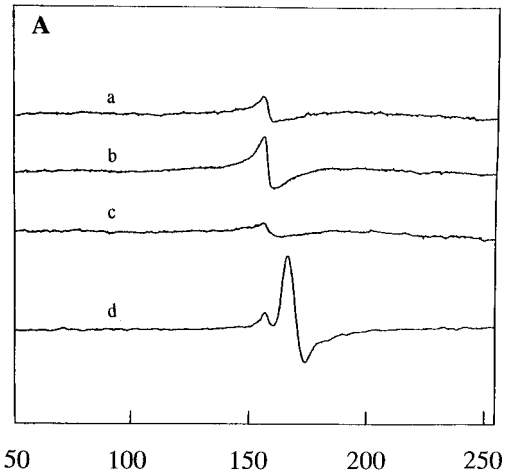

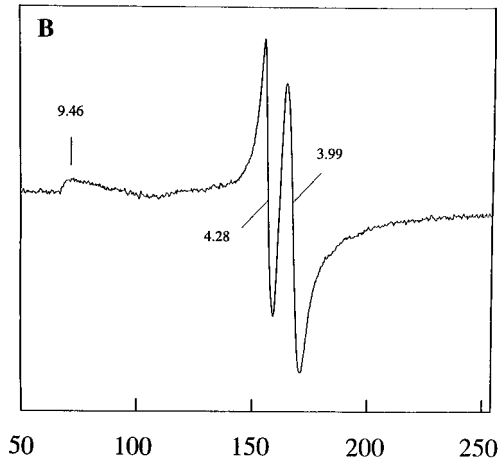

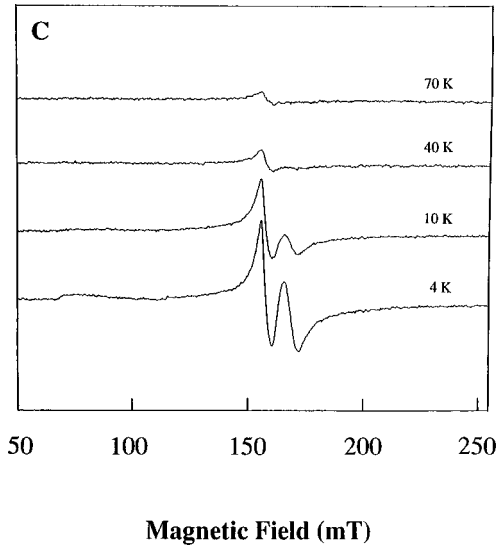

FIG. 3. EPR spectra of ES-1 ADH. (A) ADH was used at a concentration of 3.2 mg/ml. The samples were as follows: ADH as isolated in 50 mM Tris-HCl (pH 8.0) containing 10% (vol/vol) glycerol and 2 mM dithiothreitol (a), the pure enzyme after the addition of excess 2,6-dichlorophenol indophenol (b), the pure enzyme after the addition of 5 mM sodium dithionite (c), and the dithionite-reduced enzyme after bubbling with NO for 3 min at 25°C prior to freezing in liquid N_2 (d). Spectra were recorded at 4 K with 5 mW of microwave power. (B and C) ADH treated with NO. The enzyme (14 mg/ml in 50 mM Tris-HCl [pH 8.0]) was gently bubbled with NO for 3 min at 25°C prior to being frozen in liquid N_2 for EPR analysis. The spectra were recorded with 5 mW of microwave power at 4 K (B) or with 1 mW of microwave power at the indicated temperatures (C). The spectrometer settings were as follows: microwave frequency, 9.442 GHz; modulation frequency, 100 kHz; modulation amplitude, 5 G; time constant, 163.84 ms; gain, 5×10^4; and scale, 15.

mobilis (ADHII [49, 63]) and *E. coli* (adhE [26, 33]) have been shown to be iron dependent, and in both cases the metal is lost during purification (32, 49). *Z. mobilis* ADH is a homotetramer (M_r of 150,000), like the ES-1 and *T. litoralis* enzymes, but it utilizes only ethanol as a substrate. In contrast, the *E. coli* adhE protein is a homopolymeric multienzyme complex (subunit M_r of 96,000) that has pyruvate formate lyase deactivase and acetyl-CoA reductase, as well as ADH, activities (19, 32, 33). The evolutionary relationships between these mesophilic enzymes and the hyperthermophilic ADHs must obviously await the complete sequencing of the latter type of enzyme. Nevertheless, ES-1 ADH represents the most stable ADH yet known. For example, ADH from *S. solfataricus* (T_{max}, 87°C) has a half-life at 70°C of 5 h (55). This compares with a half-life for ES-1 ADH at 85°C of 35 h (35, 41).

EPR analyses indicated that ES-1 ADH contains a mononuclear iron site, but in the pure enzyme this exists in a mixture of ferric and ferrous forms. The presence of ferrous iron was substantiated by treating the enzyme with NO, which yielded EPR spectra from a putative ferrous NO complex. The same procedure was used previously to identify EPR-silent ferrous sites in lipoxygenase (17, 58) and catecholic dioxygenases (5, 76). Only three other enzymes that contain monomeric iron sites, phenylalanine monooxygenase (25), superoxide dismutase (8, 70), and nitrile hydratase (31, 67), are known to exist. The latter two enzymes and intradiol-type catecholic dioxygenases (37) contain a ferric center, while extradiol dioxygenases (76), lipoxygenases (17), phenylalanine monooxygenase (72), and ADH of *Z. mobilis* (6, 69) contain high-spin

TABLE 5. Substrate specificity of ES-1 ADH

Substrate[a]	Activity (%)[b]
Methanol	0
Ethanol	100
1-Propanol	102
2-Propanol	0
1-Butanol	130
Isobutanol	93
4-Hydroxylbutyric acid	0
1-Pentanol	135
1-Hexanol	165
1-Heptanol	114
1-Octanol	64
1,3-Propanediol	6
2-Phenyl ethanol	70
Tryptophol	20
Glycerol	0
D-Sorbitol	0

[a] All substrates were used at a concentration of 60 mM.
[b] One hundred percent activity equals 54 U/mg at 80°C.

TABLE 6. Kinetic parameters of ADH from ES-1

Substrate (concn [mM])	Cosubstrate (concn [mM])	Apparent K_m (mM)	Apparent V_{max} (U/mg)	k_{cat}/K_m (mM^{-1} s^{-1})
Ethanol (7.2–48)	NADP (0.3)	8.0	62	6.0
Acetaldehyde (0.13–4.0)	NADPH (0.3)	0.25	25	76.4
2-Phenyl ethanol (10–100)	NADP (0.4)	15	42	2.1
Phenylacetaldehyde (0.13–2.5)	NADPH (0.15)	0.05	20	300
Tryptophol (1.25–10)	NADP (0.3)	6.3	23	2.8
NADP (0.025–0.4)	Ethanol (72)	0.014	55	2,990
NADPH (0.05–0.3)	Acetaldehyde (0.5)	0.042	19	345
NAD (0.05–0.5)	Ethanol (60)	≥10	42	<3.2

ferrous sites (S = 2). Additional spectroscopic studies will be needed to ascertain the spin state of the ferrous site in ES-1 ADH. The catalytic role of this site is also unclear, but it appears to have a very high reduction potential and it is probably not redox active during the catalytic cycle. Moreover, the pure enzyme (containing Fe^{2+} and Fe^{3+}) and the dithionite-reduced enzyme (predominantly Fe^{2+}) were equally active. The weak visible absorption of pure ADH presumably arises from the ferric form of the enzyme (17, 37, 46). Spectroscopic analyses of *Z. mobilis* ADH have indicated that its mononuclear metal site is coordinated by three to four histidine ligands with two or three O ligands supplied by H_2O or acidic residues (6, 69). Three histidinyl residues also coordinate the monomeric iron site of superoxide dismutase (66) and lipoxygenase (14). *T. litoralis* ADH contains only one histidinyl residue per monomer (Table 4), and so it remains to be seen whether the higher histidine content of ES-1 ADH (eight residues per monomer) is related to this enzyme's ability to retain iron during purification.

We have shown here that the growth of ES-1, as with several other hyperthermophilic archaea (2, 65), is obligately dependent upon the presence of S^0 in the growth medium, although this is in contrast to what was previously reported (53). ES-1 appears to obtain energy for growth by coupling the oxidation of protein-derived amino acids ultimately to the reduction of S^0 to H_2S. Presumably, energy is conserved by substrate-level phosphorylation and by S^0 respiration (52, 60). The direct oxidation of peptide-derived amino acids by dehydrogenase-type enzymes is not a major catabolic route in ES-1, as cell extracts were found to contain very low activities of AlaDH, ValDH, LeuDH, and PheDH. Rather, transamination-type reactions appear to produce the corresponding 2-keto acid from amino acids with transfer of the amino group to 2-ketoglutarate to generate glutamate. This is supported by the presence of high GDH activity in cell extracts (Table 2), which regenerates 2-ketoglutarate from glutamate. ES-1 also contains four distinct ferredoxin-linked keto acid oxidoreductase activities (Table 2). In combination, these oxidatively decarboxylate the transaminated forms of most of the amino acids. The corresponding acyl- or aryl-CoA derivatives can be used for energy conservation. Previous studies have shown that the hyperthermophilic archaea contain the enzyme acetyl-CoA synthetase (ADP utilizing) (59). This enzyme converts acetyl-CoA, ADP, and phosphate to acetate and ATP in a single step, in contrast to the two-step process in mesophilic bacteria (68). Since both acetate and isovalerate are major products of the growth of ES-1, we assume that acetyl-CoA synthetase also utilizes other keto acid derivatives.

The proposed pathway for amino acid to organic acid conversion in ES-1, wherein the excess reductant both from the GDH reaction (as NADPH) and 2-keto acid oxidation (as reduced ferredoxin) is utilized for H_2S production, is shown in Fig. 4. We have shown here that in S^0-sufficient media, the activities of ADH and hydrogenase are barely detectable in ES-1 and little if any alcohol or H_2 is produced. When growth was limited by S^0, however, the specific activities of ADH and hydrogenase (and also FMOR) increased dramatically (Table 2), and H_2 and alcohol (ethanol and butanol) production increased by 20- and 4-fold, respectively (Table 1). The increased activity of ADH is most easily explained by its use in the disposal of reductant. Under S^0-limiting conditions, the production of both NADPH and reduced ferredoxin presumably exceeds the amounts that can be oxidized by S^0 reduction, and some of the excess reductant is disposed of as alcohol (Fig. 4). Consequently, S^0-limited cells contain significant ADH activity, and the enzyme is kinetically predisposed to reduce aldehydes rather than to oxidize alcohols. The question then becomes what is the source of the aldehydes that are used as substrates by ADH?

Table 1 shows that ES-1 contains significant activities of two aldehyde-oxidizing enzymes, AOR (47), which has a broad substrate range, and FOR (48), which oxidizes only C_1 to C_3 aliphatic aldehydes. These enzymes might function in the reverse direction to produce aldehydes with concomitant oxidation of reduced ferredoxin. However, ES-1 AOR was recently purified, and from kinetic analyses it was concluded that the reduction of organic acids is unlikely to be the physiological reaction (28). Moreover, the most efficient aldehyde substrates for ES-1 AOR were acetaldehyde, isovalerylaldehyde, and phenylacetaldehyde, which are derivatives of the substrates for the keto acid oxidoreductases found in ES-1 (Table 1). To investigate whether these aldehydes could be generated from these 2-keto acids as side products of the keto acid oxidoreductase reaction, we used POR and ferredoxin purified from *P. furiosus* (11). Surprisingly, under standard assay conditions at 80°C (11), the production of 720 μM acetyl-CoA was accom-

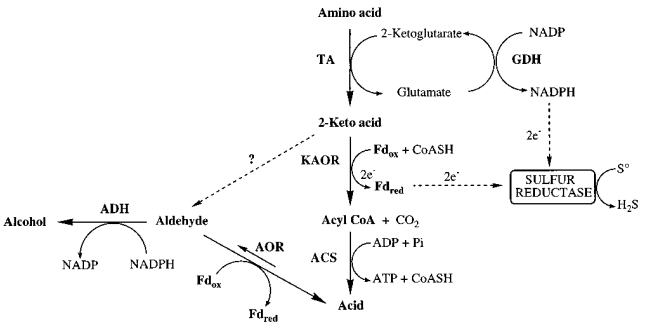

FIG. 4. General scheme for amino acid oxidation in ES-1 and the proposed metabolic role of ADH. Abbreviations: TA, transaminases; KAOR, 2-keto acid oxidoreductases; ACS, acetyl-CoA synthetase; Fd_{ox}, oxidized ferredoxin; Fd_{red}, reduced ferredoxin.

panied by the accumulation of 80 μM acetaldehyde, as measured by NADP production catalyzed by ES-1 ADH (40). Thus, although these analyses have to be substantiated under a variety of reaction conditions, it does appear that aldehydes are produced by the POR reaction at 80°C, and presumably the same is true for VOR and IOR (Table 1). Assuming that this also occurs in vivo, we suggest that it is these aldehydes which are reduced by ADH to the corresponding alcohol. Notably, both acetaldehyde and phenylacetaldehyde are excellent substrates for ADH (Table 6). We therefore propose (Fig. 4) that under S^0-sufficient conditions, the aldehydes produced from 2-keto acids are oxidized by AOR with the production of reduced ferredoxin (28) but that under conditions of S^0 limitation, these aldehydes are reduced by ADH. Reduction of aldehydes by ADH rather than their oxidation by AOR generates an oxidized electron carrier (NADP) rather than a reduced one (reduced ferredoxin). This tentative scheme for amino acid-to-alcohol conversion (Fig. 4) should be interpreted with caution, however, as several aspects remain to be explained. For example, the possibility that the physiological function of AOR is acid reduction cannot be ruled out, and it is difficult to understand why ADH (and also FMOR) is present in such apparently large amounts in S^0-limited cells. Also, it has yet to be conclusively established that 2-keto acids are the primary source of the aldehydes that serve as substrates for ADH.

In addition to its effect on ADH, S^0-limited growth of ES-1 resulted in dramatic increases in the activities of FMOR, a ferredoxin-linked enzyme which reversibly converts formate to CO_2, and hydrogenase. We assume that, like ADH, both of these enzymes are involved in disposing of the excess reductant that would otherwise accumulate under S^0 limitation (27, 43). In any event, the dependence of the growth of ES-1 on S^0 availability appears to be a result mainly of the organism's inability to efficiently dispose of the reductant generated during amino acid oxidation. S^0 limitation presumably results in an increased ratio of reduced to oxidized electron carriers, and it is this change that leads to the increase in the activities of ADH, FMOR, and hydrogenase, rather than a direct role of S^0, sulfide, or polysulfide. This situation is probably analogous to the anaerobic regulation of *E. coli* (36). As far as we are aware, the three enzymes ADH, hydrogenase, and FMOR of *Thermococcus* strain ES-1 are the first whose regulation depends upon the availability of S^0 in a growth medium.

ACKNOWLEDGMENTS

This research was supported by grants from the National Science Foundation (BCS-9320069) and the Office of Naval Research (N00014-90-J-1894).

REFERENCES

1. **Adams, M. W. W.** 1993. Enzymes and proteins from organisms that grow near and above 100°C. Annu. Rev. Microbiol. **47:**627–658.
2. **Adams, M. W. W.** 1994. Biochemical diversity among sulfur-dependent hyperthermophilic microorganisms. FEMS Microbiol. Rev. **15:**267–277.
3. **Ammendola, S., C. A. Raia, C. Caruso, L. Camardella, S. D'Auria, M. De Rosa, and M. Rossi.** 1992. Thermostable NAD-dependent alcohol dehydrogenase from *Sulfolobus solfataricus* gene and protein sequence determination and relationship to other alcohol dehydrogenases. Biochemistry **31:**12514–12523.
4. **Aono, S., F. O. Bryant, and M. W. W. Adams.** 1989. A novel and remarkably thermostable ferredoxin from the hyperthermophilic archaebacterium *Pyrococcus furiosus*. J. Bacteriol. **171:**3433–3439.
5. **Arciero, D. M., A. M. Orville, and J. D. Lipscomb.** 1985. ^{17}O-water and nitric oxide binding by protocatechuate 4,5 dioxygenase and catechol 2,3 dioxygenase. J. Biol. Chem. **260:**14035–14044.
6. **Bakshi, E. N., P. Tse, K. S. Murray, G. R. Hanson, R. K. Scopes, and A. G. Wedd.** 1989. Iron-activated alcohol dehydrogenase from *Zymomonas mobilis*: spectroscopic and magnetic properties. J. Am. Chem. Soc. **189:**8707–8713.
7. **Baross, J. A.** Personal communication.
8. **Barrette, W. C., Jr., D. T. Sawyer, J. A. Fee, and K. Asada.** 1983. Potentiometric titrations and oxidation-reduction potentials of several iron superoxide dismutases. Biochemistry **22:**624–627.
9. **Bennetzen, J. L., and B. D. Hall.** 1982. The primary structure of the *Saccharomyces cerevisiae* gene for alcohol dehydrogenase I. J. Biol. Chem. **257:**3018–3025.
10. **Blamey, J. M., and M. W. W. Adams.** 1993. Purification and characterization of pyruvate ferredoxin oxidoreductase from the hyperthermophilic archaeon, *Pyrococcus furiosus*. Biochem. Biophys. Acta **1161:**19–27.
11. **Blamey, J. M., and M. W. W. Adams.** 1994. Characterization of an ancestral-type of pyruvate ferredoxin oxidoreductase from the hyperthermophilic bacterium, *Thermotoga maritima*. Biochemistry **33:**1000–1007.
12. **Bleicher, K., and J. Winter.** 1991. Purification and properties of F_{420}- and NADP-dependent alcohol dehydrogenases of *Methanogenium liminatans* and *Methanobacterium palustre*, specific for secondary alcohols. Eur. J. Biochem. **200:**43–51.
13. **Blumentals, I. I., M. Itoh, G. J. Olson, and R. M. Kelly.** 1990. Role of polysulfides in reduction of elemental sulfur by the hyperthermophilic archaebacterium *Pyrococcus furiosus*. Appl. Environ. Microbiol. **56:**1255–1262.
14. **Boyington, J. C., B. J. Gaffney, and L. M. Amzel.** 1993. The three-dimensional structure of an arachidonic acid 15-lipoxygenase. Science **260:**1482–1486.
15. **Bradford, M. M.** 1976. A rapid and sensitive method for the quantitation of microgram quantities of protein utilizing the principle of protein-dye binding. Anal. Biochem. **72:**248–254.
16. **Bryant, F. O., and M. W. W. Adams.** 1989. Characterization of hydrogenase from the hyperthermophilic archaebacterium, *Pyrococcus furiosus*. J. Biol. Chem. **264:**5070–5079.
17. **Chasteen, N. D., J. K. Grady, K. I. Skorey, K. J. Neden, D. Riendeau, and M. D. Percival.** 1993. Characterization of the non-heme iron center of human 5-lipoxygenase by electron paramagnetic resonance, fluorescence, and ultraviolet-visible spectroscopy: redox cycling between ferrous and ferric states. Biochemistry **32:**9763–9771.
18. **Chen, J.-S., and L. E. Mortenson.** 1977. Inhibition of methylene blue formation during determination of acid-labile sulfide of iron-sulfur protein samples containing dithionite. Anal. Biochem. **79:**157–165.
19. **Clarke, D. P.** 1989. The fermentation pathways of *Escherichia coli*. FEMS Microbiol. Rev. **63:**223–234.
20. **Deutscher, M. P.** 1990. Guide to protein purification. Methods Enzymol. **182:**588–604.
21. **Drewke, C., and M. Ciriacy.** 1988. Overexpression, purification and properties of alcohol dehydrogenase IV from *Saccharomyces*. Biochim. Biophys. Acta **950:**54–60.
22. **Edelhoch, H.** 1967. Spectroscopic determination of tryptophan and tyrosine in protein. Biochemistry **6:**1948–1954.
23. **Fiala, G., and K. O. Stetter.** 1986. *Pyrococcus furiosus* sp. nov. represents a novel genus of marine heterotrophic archaebacteria growing optimally at 100°C. Arch. Microbiol. **145:**56–61.
24. **Fischer, R. J., J. Helms, and P. Dürre.** 1993. Cloning, sequencing, and molecular analysis of the *sol* operon of *Clostridium acetobutylicum*, a chromosomal locus involved in solventogenesis. J. Bacteriol. **175:**6959–6969.
25. **Fisher, D. B., R. Kirkwood, and S. Kaufman.** 1972. Rat liver phenylalanine hydroxylase, an iron enzyme. J. Biol. Chem. **247:**5161–5167.
26. **Goodlove, P. E., S. M. Bury, and L. Sawyer.** 1989. Cloning and sequence analysis of the fermentative alcohol-dehydrogenase-encoding gene of *Escherichia coli*. Gene **85:**209–214.
27. **Heider, J., and M. W. W. Adams.** Unpublished data.
28. **Heider, J., K. Ma, and M. W. W. Adams.** 1995. Purification, characterization, and metabolic function of tungsten-containing aldehyde ferredoxin oxidoreductase from the hyperthermophilic and proteolytic archaeon *Thermococcus* strain ES-1. J. Bacteriol. **177:**4757-4764.
29. **Heider, J., X. Mai, and M. W. W. Adams.** Unpublished data.
30. **Hensgens, C. M., J. Vonck, J. van Beeumen, E. F. J. van Bruggen, and T. A. Hansen.** 1993. Purification and characterization of an oxygen-labile, NAD-dependent alcohol dehydrogenase from *Desulfovibrio gigas*. J. Bacteriol. **175:**2859–2863.
31. **Jin, H., I. M. Turner, Jr., M. J. Nelson, R. J. Gurbiel, P. E. Doan, and B. M. Hoffman.** 1993. Coordination sphere of the ferric ion in nitrile hydratase. J. Am. Chem. Soc. **115:**5290–5291.
32. **Kessler, D., W. Herth, and J. Knappe.** 1992. Ultrastructure and pyruvate-quenching property of the multienzyme AdhE protein of *Escherichia coli*. J. Biol. Chem. **267:**18073–18079.
33. **Kessler, D., I. Leibrecht, and J. Knappe.** 1991. Pyruvate-formate-lyase-deactivase and acetyl-CoA reductase activities of *Escherichia coli* reside on a polymeric operon particle encoded by *adhE*. FEBS Lett. **281:**59–63.
34. **Laemmli, U. K.** 1970. Cleavage of structural proteins during the assembly of the head bacteriophage T4. Nature (London) **227:**680–685.
35. **Lamed, R. J., and J. G. Zeikus.** 1981. Novel NADP-linked alcohol-aldehyde/ketone oxidoreductase in thermophilic ethanogenic bacteria. Biochem. J. **195:**183–190.
36. **Leonardo, M. R., P. R. Cunningham, and D. P. Clark.** 1993. Anaerobic

regulation of the *adhE* gene, encoding the fermentative alcohol dehydrogenase of *Escherichia coli*. J. Bacteriol. **175:**870–878.
37. **Lipscomb, J. D., and A. M. Orville.** 1992. Mechanistic aspects of dihydroxybenzoate dioxygenases, p. 243–298. *In* H. Sigel and A. Sigel (ed.), Metal ions in biological systems, vol. 28. Marcel Dekker, New York.
38. **Lovenberg, W., B. B. Buchanan, and J. C. Rabinowitz.** 1963. Studies on the chemical nature of ferredoxin. J. Biol. Chem. **238:**3899–3913.
39. **Ma, K., and M. W. W. Adams.** 1994. Sulfide dehydrogenase from the hyperthermophilic archaeon *Pyrococcus furiosus*: a new multifunctional enzyme involved in the reduction of elemental sulfur. J. Bacteriol. **176:**6509–6517.
40. **Ma, K., and M. W. W. Adams.** Unpublished data.
41. **Ma, K., F. T. Robb, and M. W. W. Adams.** 1994. Purification and characterization of NADP-specific alcohol dehydrogenase and NADP-specific glutamate dehydrogenase from the hyperthermophilic archaeon *Thermococcus litoralis*. Appl. Environ. Microbiol. **60:**562–568.
42. **Ma, K., R. N. Schicho, R. M. Kelly, and M. W. W. Adams.** 1993. Hydrogenase of the hyperthermophile *Pyrococcus furiosus* is an elemental sulfur reductase or sulfhydrogenase: evidence for a sulfur-reducing hydrogenase ancestor. Proc. Natl. Acad. Sci. USA **90:**5341–5344.
43. **Ma, K., Z. H. Zhou, and M. W. W. Adams.** 1994. Hydrogen production from pyruvate by enzymes purified from the hyperthermophilic archaeon, *Pyrococcus furiosus*: a key role for NADPH. FEMS Microbiol. Lett. **122:**263–266.
44. **Mai, X., and M. W. W. Adams.** 1993. Characterization of aromatic and aliphatic 2-ketoacid oxidoreductases from hyperthermophilic archaea. J. Inorg. Chem. **51:**459.
45. **Mai, X., and M. W. W. Adams.** 1994. Indolepyruvate ferredoxin oxidoreductase from the hyperthermophilic archaeon, *Pyrococcus furiosus*: a new enzyme involved in peptide fermentation. J. Biol. Chem. **269:**16726–16732.
46. **Marota, J. J. A., and R. Shiman.** 1984. Stoichiometric reduction of phenylalanine hydroxylase by its cofactor: a requirement for enzyme activity. Biochemistry **23:**1303–1311.
47. **Mukund, S., and M. W. W. Adams.** 1991. The novel tungsten-iron-sulfur protein of the hyperthermophilic archaebacterium, *Pyrococcus furiosus*, is an aldehyde ferredoxin oxidoreductase: evidence for its participation in a unique glycolytic pathway. J. Biol. Chem. **266:**14208–14216.
48. **Mukund, S., and M. W. W. Adams.** 1993. Characterization of a novel tungsten-containing formaldehyde ferredoxin oxidoreductase from the extremely thermophilic archaeon, *Thermococcus litoralis*. A role for tungsten in peptide catabolism. J. Biol. Chem. **268:**13592–13600.
49. **Neale, A. D., R. K. Scope, J. M. Kelly, and R. E. H. Wettenhall.** 1986. The two alcohol dehydrogenases of *Zymomonas mobilis*—purification by different dye ligand chromatography, molecular characterization and physiological roles. Eur. J. Biochem. **154:**119–124.
50. **Neuner, A., H. Jannasch, S. Belkin, and K. O. Stetter.** 1990. *Thermococcus litoralis* sp. nov.: a new species of extremely thermophilic marine archaebacteria. Arch. Microbiol. **153:**205–207.
51. **Peretz, M., and Y. Burstein.** 1989. Amino acid sequence of alcohol dehydrogenase from the thermophilic bacterium *Thermoanaerobium brockii*. Biochem. J. **28:**6549–6555.
52. **Pihl, T. D., L. K. Black, B. A. Schulman, and R. J. Maier.** 1992. Hydrogen-oxidizing electron transport components in the hyperthermophilic archaebacterium *Pyrodictium brockii*. J. Bacteriol. **174:**137–143.
53. **Pledger, R. J., and J. Baross.** 1989. Characterization of an extremely thermophilic archaebacterium isolated from a black smoker polychaete (*Paralvinella*, *sp*.) at the Juan de Fuca Ridge. Syst. Appl. Microbiol. **12:**249–256.
54. **Reid, M. F., and C. A. Fewson.** 1994. Molecular characterization of microbial alcohol dehydrogenases. Crit. Rev. Microbiol. **20:**13–56.
55. **Rella, R., C. A. Raia, M. Pensa, F. M. Pisani, A. Gambacorta, M. De Rosa, and M. Rossi.** 1987. A novel archaebacterial NAD-dependent alcohol dehydrogenase: purification and properties. J. Biochem. **167:**475–479.
56. **Riddles, P. W., R. L. Blakeley, and B. Zerner.** 1983. Reassessment of Ellman's reagent. Methods Enzymol. **91:**49–60.
57. **Robb, F. T., J.-B. Park, and M. W. W. Adams.** 1992. Characterization of an extremely thermostable glutamate dehydrogenase: a key enzyme in the primary metabolism of the hyperthermophilic archaebacterium, *Pyrococcus furiosus*. Biochim. Biophys. Acta **1120:**267–272.
58. **Salerno, J. C., and J. N. Siedow.** 1979. The nature of the nitric oxide complexes of lipoxygenase. Biochim. Biophys. Acta **579:**246–251.
59. **Schäfer, T., M. Selig, and P. Schönheit.** 1993. Acetyl CoA synthetase (ADP-forming) in archaea, a novel enzyme involved in acetate formation and ATP synthesis. Arch. Microbiol. **159:**72–83.
60. **Schauder, R., and A. Kröger.** 1993. Bacterial sulfur respiration. Arch. Microbiol. **159:**491–497.
61. **Schauder, R., and E. Müller.** 1993. Polysulfide as a possible substrate for sulfur-reducing bacteria. Arch. Microbiol. **160:**377–382.
62. **Schicho, R. N., K. Ma, M. W. W. Adams, and R. M. Kelly.** 1993. Bioenergetics of sulfur reduction in the hyperthermophilic archaeon *Pyrococcus furiosus*. J. Bacteriol. **175:**1823–1830.
63. **Scopes, R. K.** 1983. An iron-activated alcohol dehydrogenase. FEBS Lett. **156:**303–306.
64. **Stetter, K. O.** 1986. Diversity of extremely thermophilic archaebacteria, p. 39–74. *In* T. D. Brock (ed.), The thermophiles: general, molecular, and applied microbiology. John Wiley, New York.
65. **Stetter, K. O., G. Fiala, G. Huber, R. Huber, and G. Segerer.** 1990. Hyperthermophilic microorganisms. FEMS Microbiol. Rev. **75:**117–124.
66. **Stoddard, B. L., P. L. Howell, D. Ringe, and G. A. Petsko.** 1990. The 2.1-Å resolution structure of iron superoxide dismutase from *Pseudomonas ovalis*. Biochemistry **29:**8885–8893.
67. **Sugiura, Y., and J. Kuwahara.** 1987. Nitrile hydratase: the first non-heme iron enzyme with a typical low-spin Fe(III)-active center. J. Am. Chem. Soc. **109:**5848–5850.
68. **Thauer, R. K., K. Jungermann, and K. Decker.** 1977. Energy conservation in chemotrophic anaerobic bacteria. Bacteriol. Rev. **41:**100–180.
69. **Tse, P., R. K. Scopes, and A. G. Wedd.** 1988. An iron-activated alcohol dehydrogenase: metal dissociation constants and magnetic and spectroscopic properties. J. Am. Chem. Soc. **110:**1295–1297.
70. **Verhagen, M. F. J. M., E. T. M. Meussen, and W. R. Hagen.** On the reduction potentials of Fe and Cu-Zn containing superoxide dismutases. Biochim. Biophys. Acta, in press.
71. **Villarroya, A., E. Juan, B. Egestad, and H. Joenvall.** 1989. The primary structure of alcohol dehydrogenase from *Drosophila lebanonensis*: intensive variation within insect 'short-chain' alcohol dehydrogenase lacking zinc. Eur. J. Biochem. **180:**191–197.
72. **Wallick, D. E., L. M. Bloom, B. J. Gaffney, and S. J. Benkovic.** 1984. Reductive activation of phenylalanine hydroxylase and its effect on the redox state of the non-heme iron. Biochemistry **23:**1295–1302.
73. **Walter, K. A., G. N. Bennett, and E. T. Papoutsakis.** 1992. Molecular characterization of two *Clostridium acetobutylicum* ATCC 824 butanol dehydrogenase isoenzyme genes. J. Bacteriol. **174:**7149–7158.
74. **Widdel, F., and R. S. Wolfe.** 1989. Expression of secondary alcohol dehydrogenase in methanogenic bacteria and purification of the F_{420}-specific enzyme from *Methanogenium thermophilum* strain TCI. Arch. Microbiol. **152:**322–328.
75. **Woese, C. R., O. Kandler, and M. L. Wheelis.** 1990. Towards a natural system of organisms: proposal for the domains of Archaea, Bacteria and Eucarya. Proc. Natl. Acad. Sci. USA **87:**4576–4579.
76. **Wolgel, S. A., J. E. Dege, P. E. Perkins-Olson, C. H. Juarez-Garcia, R. L. Crawford, E. Münck, and J. D. Lipscomb.** 1993. Purification and characterization of protocatechuate 2,3-dioxygenase from *Bacillus macerans*: a new extradiol catecholic dioxygenase. J. Bacteriol. **175:**4414–4426.